

# Cold fingers in a hot magma: Numerical modeling of country-rock diapirs in the Bushveld Complex, South Africa

Taras V. Gerya\* Institut of Geology, Mineralogy and Geophysics, Ruhr-University Bochum, 44780 Bochum, Germany, and  
Institute of Experimental Mineralogy, Russian Academy of Sciences, 142432 Chernogolovka, Moscow,  
Russia

Ron Uken }  
Jürgen Reinhardt }  
Michael K. Watkeys } School of Geological and Computer Science, University of Natal, Durban, 4041, South Africa

Walter V. Maresch Institut of Geology, Mineralogy and Geophysics, Ruhr-University Bochum, 44780 Bochum, Germany  
Brendan M. Clarke Council for Geoscience, P.O. Box 900, 3200, Pietermaritzburg, South Africa

## ABSTRACT

Partially molten diapirs and domes in Earth's continental crust can be an effective means of transporting heat from lower to higher levels, often producing pronounced prograde metamorphic aureoles. Our numerical thermomechanical models show that this classical thermal scenario is violated by the diapirs of partially molten metasedimentary rocks to 8 km in diameter that penetrate the Bushveld Complex, the world's largest layered intrusion. Here, diapirism was triggered by the emplacement of an 8-km-thick, hot, and dense mafic magma over a cold and less dense sedimentary succession. These diapirs promoted cooling of the giant magma chamber, bringing cooler material into higher crustal levels. Comparison between numerical results and geological observations indicates that diapir nucleation is crucially dependent on the presence of initial topographic disturbances between 800 and 1000 m in height in the floor of the magma chamber, and also allows critical parameters of initial geometry and temperature distribution of the Bushveld event to be outlined.

**Keywords:** diapirism, numerical modeling, Bushveld Complex, partial melting, plumes, subduction zones.

## INTRODUCTION

Diapirs and domes on a scale of meters to kilometers are widespread in Earth's continental crust (Ramberg, 1981) and represent an important tectonic element of cratons, orogenic belts, and sedimentary basins. These structures bring heat from lower to higher crustal levels and often produce pronounced prograde contact-metamorphic aureoles. Consequently, the existence of a positive thermal anomaly within such a rising structure is the expected thermal norm. Here we use coupled thermo-mechanical numerical modeling to show that diapirs of metasedimentary rocks found in the Bushveld Complex (Uken and Watkeys, 1997) were actually characterized by a 200–300 °C negative thermal anomaly at the time of emplacement.

## GEOLOGIC SETTING

Heat released from the world's largest layered intrusion, the ca. 2.0 Ga. Bushveld Complex, produced a contact-metamorphic aureole that extends to a present-day depth of >5 km into the underlying Transvaal Supergroup. Deformed Transvaal Supergroup rocks within the layered intrusion have been attributed to var-

ious mechanisms, but a strong case has been made for their origin as diapirs of contact-metamorphosed country rock rising through the intrusion (Uken and Watkeys, 1997).

The Rustenburg Layered Suite of the Bushveld Complex consists of a sill-shaped sequence of mafic-ultramafic rocks to 8 km thick (Du Plessis and Kleynwegt, 1987; Cawthorn et al., 1998) emplaced along the contact between the sedimentary Pretoria Group and the overlying volcanic Rooiberg Group of the Transvaal Supergroup, both ~5 km in thickness. Subsidence of the intrusion produced the present lopolithic geometry (Fig. 1A). The Rustenburg Layered Suite is subdivided from bottom to top into the lower, critical, main, and upper zones (Fig. 1B). The lower zone occurs as separate compartments, each of alternating bronzitite, harzburgite, and dunite (Sharpe, 1986). The critical zone oversteps the lower zone and consists mainly of norites, leuconorites, and anorthosites that host economically important chromite and platiniferous horizons. The main zone is a thick succession of dominantly gabbro, followed by the upper zone, which comprises ferrogabbros with cumulus magnetite layers.

The floor of the Rustenburg Layered Suite consists of contact-metamorphosed Pretoria

Group shales and sandstones with minor carbonate and volcanoclastic rocks. These in turn overlie banded ironstone and dolomite of the Chuniespoort Group of the Transvaal Supergroup, mostly unaffected by metamorphism and associated deformation. The outermost parts of the aureole are characterized by metapelitic assemblages of chloritoid and biotite, followed by a wide andalusite zone with staurolite, garnet, or cordierite, a fibrolite-cordierite zone, and an inner zone of migmatite.

The Rooiberg Group roof rocks are dominated by felsic volcanics and volcanoclastics considered contemporaneous with the intrusion of the Rustenburg Layered Suite (Hatton and Schweitzer, 1995) and intruded by the Lebowa Granite Suite. Precise SHRIMP ages for the crystallization of the Rooiberg Group, Rustenburg Layered Suite, and Lebowa Granite Suite are statistically indistinguishable, indicating that all magmatic activity occurred within the attainable precision of 3–5 m.y. (Harmer and Armstrong, 2000). At least seven large diapiric structures of contact-metamorphosed Pretoria Group rocks penetrate the overlying Rustenburg Layered Suite (Uken and Watkeys, 1997) (Figs. 1B, 1C). Diapirs are developed above a décollement zone that corresponds approximately with the 550 °C metamorphic isotherm (Uken and Watkeys, 1997). Diapirs are irregularly spaced; the distance between diapirs averages ~30 km (Fig. 1B). Diapir outcrop shapes range between open to tight cusped-like profiles (e.g., Katkloof, Schwerin, Zaaikloof) to asymmetrical bulbous shapes with overturned and overhanging margins (e.g., Phepane) (Fig. 1C). The Malope structure represents a deformed elongated diapir head that partially penetrated the roof rocks, with limbs dipping at an average of 30°. Strongly lineated, boudinaged, and foliated Pretoria Group rocks are developed between the diapirs; fabrics show extreme loading and near-bedding-parallel extension with flow toward diapir culminations. Ponding of lower zone magmas between diapirs, trunca-

\*E-mail: taras.gerya@ruhr-uni-bochum.de.

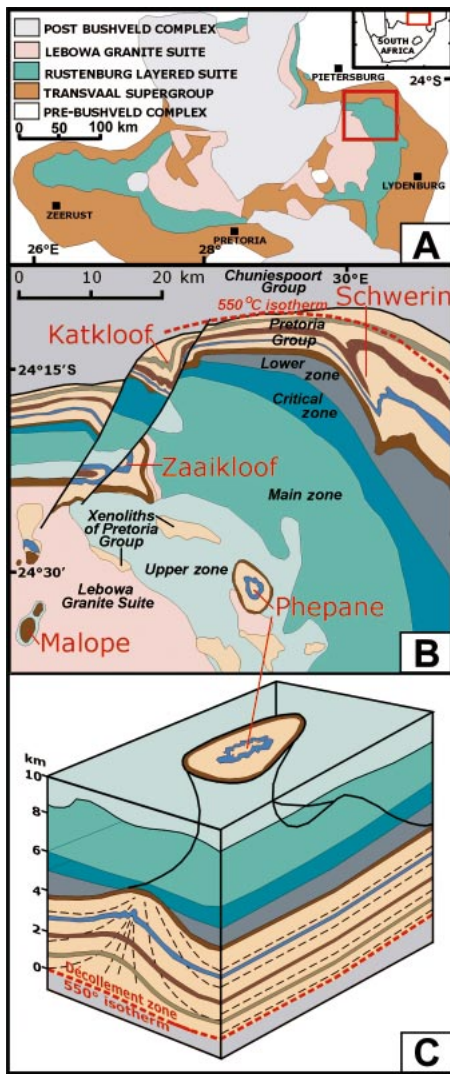


**Figure 1. Distribution and geometry of diapirs in Bushveld complex, South Africa. A: Bushveld Complex showing diapir field in northeast (red box), enlarged in B. B: Geology of diapiric area showing distribution of main diapiric structures (red labels). C: Reconstructed idealized geometry and structure of Phepane diapir (Uken and Watkeys, 1997) showing bulbous head, décollement zone, foliation traces (dashed), and 550 °C isotherm in floor.**

tion of upper zone layers by the diapirs, and thinning of the Rustenburg Layered Suite over the diapirs indicate that the diapirism was initiated in the early stages of magmatic emplacement and continued as the magma chamber thickened. Furthermore, the diapirs are causally related to the initial perturbations in the magma-chamber floor that resulted from lobate lateral advancement of lower zone magmas (Uken and Watkeys, 1997).

### NUMERICAL MODELING

Figure 2 presents the initial geometry and the development with time of our reference model (Table 1) for comparison with the principal tectonic characteristics of the diapirs developed within the Rustenburg Layered Suite. The internal geometry of the model is based on the geological, geochronological, and stratigraphic data discussed herein for the northeastern Bushveld Complex. Taking into account the average distance between diapirs, we used a 30 km characteristic lateral box size. Nucleation of a diapir is localized by the presence of an initial anticline (Uken and Wat-

keys, 1997) of small amplitude on the intrusion floor in the central part of the model. Numerical experiments were performed by using implicit finite-difference-based computer code I2 (Gerya et al., 2000), allowing a coupled thermomechanical solution of governing equations (momentum, continuity, and temperature) for viscous multiphase flow. Latent heats of melting and of crystallization processes as well as changes in density, viscosity, and heat capacity of partially molten rocks (Table 1) are accounted for by using the methodology suggested by Bittner and Schmeling (1995).

The early stages of the cooling process (0–0.5 m.y.) are characterized by massive, outward-directed heat flow from the mafic intrusion, resulting in the generation and widening of zones of partially molten rocks with lowered viscosity in both overlying felsic volcanic rocks of the Rooiberg Group and underlying sedimentary sequences of the Pretoria Group. Due to the Rayleigh-Taylor instability caused by the density contrast between the crystallizing hot mafic intrusion and the underlying felsic, partially molten sedimentary rocks, the initial anticline in the intrusion floor grows into the magma as a dome composed of contact-metamorphosed country rocks. In contrast to common crustal dome structures (Bittner and Schmeling, 1995), this feature is characterized by a 200–300 °C increase in temperature from the core toward the margins. The next stages (0.5–0.8 m.y.) are manifested by rapid transformation of the dome into an elongated diapir penetrating the Rustenburg Layered Suite intrusion and inducing cooling of the magmatic environment. This dome transformation is also associated with the development of marginal synclines at the base of the diapir, accommodating thinning of the source sedimentary sequence (cf. Figs. 1 and 2). At the culmination stage of growth, the apical part of the diapir penetrates the partially molten felsic roof sequence (cf. Figs. 1 and 2). This penetration is consistent with field relationships (Fig. 1B). The last stages of the process (1.0–6.0 m.y.) are characterized by progressive cooling of the whole crustal sequence, resulting in “freezing” of the shape of the diapir within the crystallizing mafic magmatic body. The average diapir growth rate before 1.0 m.y. is ~8 mm/yr. This growth rate is also consistent with previous estimates (Uken and Watkeys, 1997) based on geologic data.

Figure 3 illustrates the influence that changes in model parameters have on the geometry of the diapir. Diapirism is dependent on the wavelength and amplitude of the initial anticlinal disturbance. Diapirs are not developed when this amplitude is <800 m (Fig. 3A). The diapir shape also becomes incon-

TABLE 1. MATERIAL PROPERTIES USED IN 2D NUMERICAL EXPERIMENTS

| Units                                 | Rocks                  | Density, $\rho$ (kg/m <sup>3</sup> ) | Thermal conductivity (W/m/K) | Flow law, $\eta_0$ (Pa s)                              | $T_{\text{solidus}}$ (°C) | $T_{\text{liquidus}}$ (°C) | Latent heat, $H_L$ (kJ/kg) |
|---------------------------------------|------------------------|--------------------------------------|------------------------------|--|---------------------------|----------------------------|----------------------------|
| Rooiberg Group (5 km thick)           | Felsic volcanic rocks  | 2700 (solid)<br>2400 (molten)        | 2.5                          | Wet granite,<br>$5 \times 10^{14}$                     | 675                       | 925                        | 300                        |
| Rustenburg Layered Suite (8 km thick) | Mafic-ultramafic rocks | 3000 (solid)<br>2900 (molten)        | 3.5                          | Plagioclase (An <sub>75</sub> ),<br>$1 \times 10^{13}$ | 950                       | 1100                       | 380                        |
| Pretoria Group (4 km thick)           | Quartzites             | 2650 (solid)<br>2450 (molten)        | 2.5                          | Wet quartzite,<br>$5 \times 10^{14}$                   | 675                       | 925                        | 300                        |
|                                       | Pelitic rocks          | 2600 (solid)<br>2400 (molten)        | 2.5                          | Wet granite,<br>$5 \times 10^{14}$                     | 675                       | 925                        | 300                        |
|                                       | Diabases               | 3000                                 | 3.5                          | Plagioclase (An <sub>75</sub> )                        | -                         | -                          | -                          |
| Chuniespoort Group (5 km thick)       | Banded iron formation  | 3000                                 | 2.5                          | Wet quartzite  | -                         | -                          | -                          |
|                                       | Siliceous dolomites    | 2500                                 | 2.5                          | Wet quartzite  | -                         | -                          | -                          |

Note: Material properties are taken from the literature (Bittner and Schmeling, 1995; Turcotte and Schubert, 1982; Ranalli, 1995). Changes in volumetric fraction of melt with temperature —  $M = 0$  at  $T < T_{\text{liquidus}}$ ,  $M = (T - T_{\text{liquidus}})/(T_{\text{solidus}} - T_{\text{liquidus}})$ , and  $M = 1$  at  $T > T_{\text{solidus}}$ . Properties of partially molten rock are as follows (Bittner and Schmeling, 1995): Density (in kg/m<sup>3</sup>) —  $\rho_{\text{eff}} = \rho_{\text{solid}} - M(\rho_{\text{solid}} - \rho_{\text{molten}})$ ; viscosity (in Pa-s) ( $M \geq 0.1$ ) —  $\eta_{\text{eff}} = \eta_0 \exp\{2.5 + [(1 - M)/M]^{0.49}[1 - M]\}$ ; heat capacity (in J/K/kg) —  $Cp_{\text{eff}} = Cp + H_L/(T_{\text{liquidus}} - T_{\text{solidus}})$ , where  $Cp = 1000$  J/K/kg is heat capacity of solid rocks. Reference model (Fig. 2) parameters are as follows: Box size— $30 \times 22$  km; resolution— $91 \times 67$  nodes, 148,500 markers; boundary conditions—free slip (all boundaries),  $T = 25$  °C on top,  $\partial T/\partial x = 0$  on walls,  $\partial^2 T/\partial z^2 = 0$  at bottom. Initial conditions (at 0 m.y.)— $T = 25$  °C on top,  $T = 325$  °C at bottom, Rooiberg Group  $T = 25$ – $525$  °C ( $\partial T/\partial z = 100$  °C/km), Rustenburg Layered Suite  $T = 1200$  °C, Transvaal Supergroup  $225$ – $325$  °C ( $\partial T/\partial z = 11$  °C/km), height of initial anticline = 1000 m. Lower and upper limits for viscosity are  $10^{17}$  Pa-s and  $10^{25}$  Pa-s, respectively.

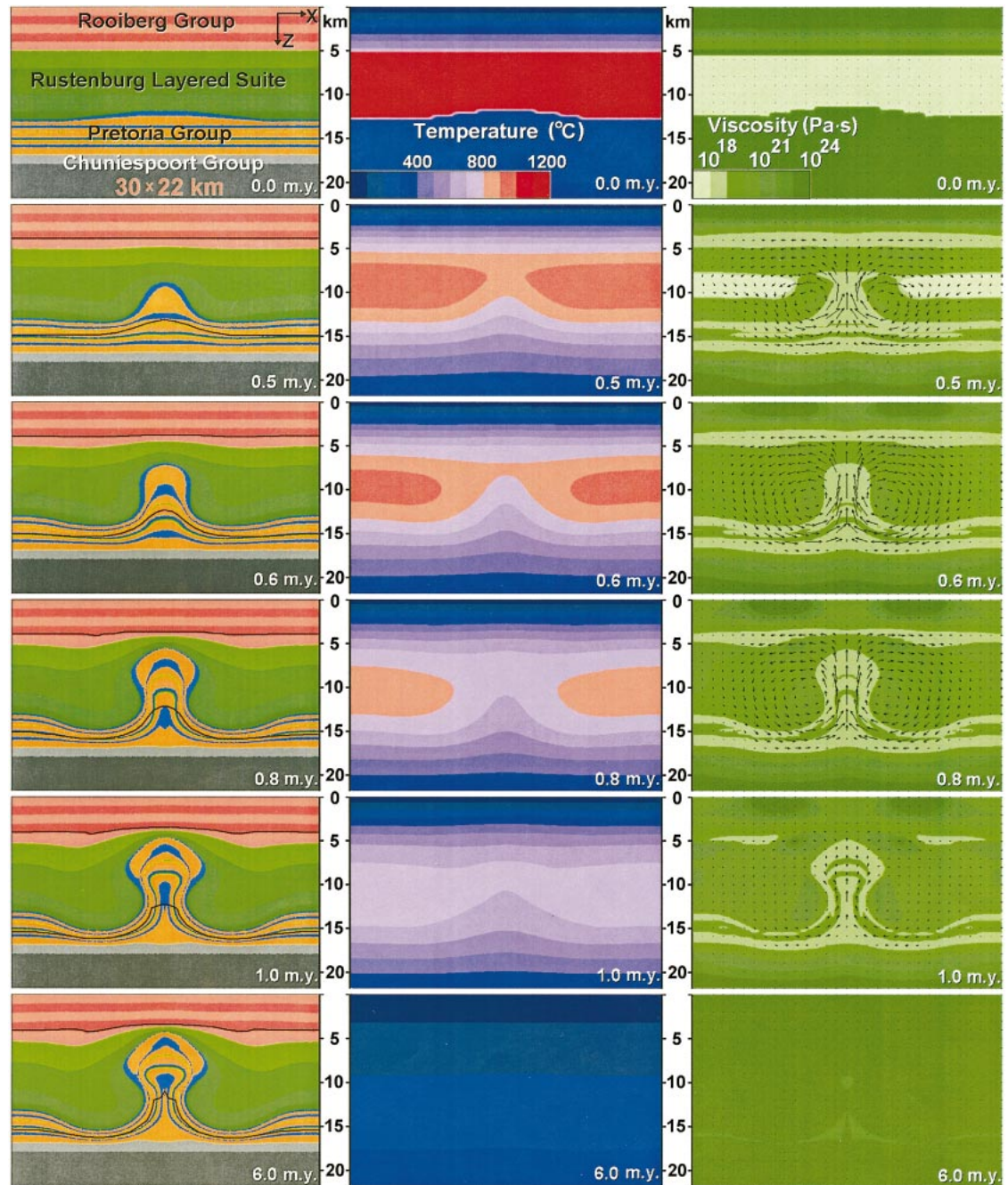


Figure 2. Results of numerical modeling showing development of diapir penetrating magma chamber. Three columns represent calculated cross-sectional changes in geometry (left), thermal structure (middle), and viscosity (right) of numerical reference model (see Table 1) with time. Solid black line in left column shows maximum extent of migmatization in felsic roof (upper line) and sedimentary floor (lower line). Lithologic structure (Uken and Watkeys, 1997), top to bottom: Rooiberg Group—felsic volcanic rocks (red); Rustenburg Layered Suite—mafic rocks of upper zone (lightest green), main zone (light green), critical zone (green), and lower zone (dark green); Pretoria Group—pelitic rocks (orange), quartzites (light blue), diabases (green); Chuniespoort Group—banded iron formation (light gray), siliceous dolomites (dark gray).

sistent with field observations (exaggerated mushroom like) when the amplitude is taken to be larger than 1000 m (Fig. 3B). Variations in the initial temperature distribution within the model (Figs. 3C–3F) also strongly affect diapir development and geometry: (1) the diapir fails to develop when there is a significant decrease in either the temperature gradient within the roof sequence (Fig. 3C) or the emplacement temperature of the Rustenburg Layered Suite (Fig. 3E); (2) the diapir shows an unrealistic mushroom-like shape (Figs. 3D, 3F) complicated by additional domal structures when there is a significant increase in those parameters. A decrease in

the characteristic lateral box size (i.e., in the characteristic size of the source area) results in a lower-amplitude and more dome-like shape of the diapir (Fig. 3G). However, an increase in the size of the source area to at least 60 km (Fig. 3H) does not significantly affect the geometry of the diapir, nor does it generate additional diapirs (cf. Fig. 3F) in the model box. This result further supports the suggestion (Uken and Watkeys, 1997) that diapir nucleation was crucially defined by the formation of initial anticline-shaped disturbances after fingered lateral injection of the lower zone between the felsic roof and sedimentary floor sequences. Due to this fin-

gered emplacement a variety of different anticlinal amplitudes and wavelengths was initially present, allowing preferential selection for diapiric growth during the cooling process.

#### DISCUSSION AND CONCLUSIONS

The cold diapirs studied here are related to the temporal inversion of a vertical temperature gradient due to the emplacement of large amounts of hot and heavy mafic magma onto a cold and less dense felsic sedimentary succession. Although this process has so far been described only from the Bushveld Complex, similar cold diapirism could have occurred in

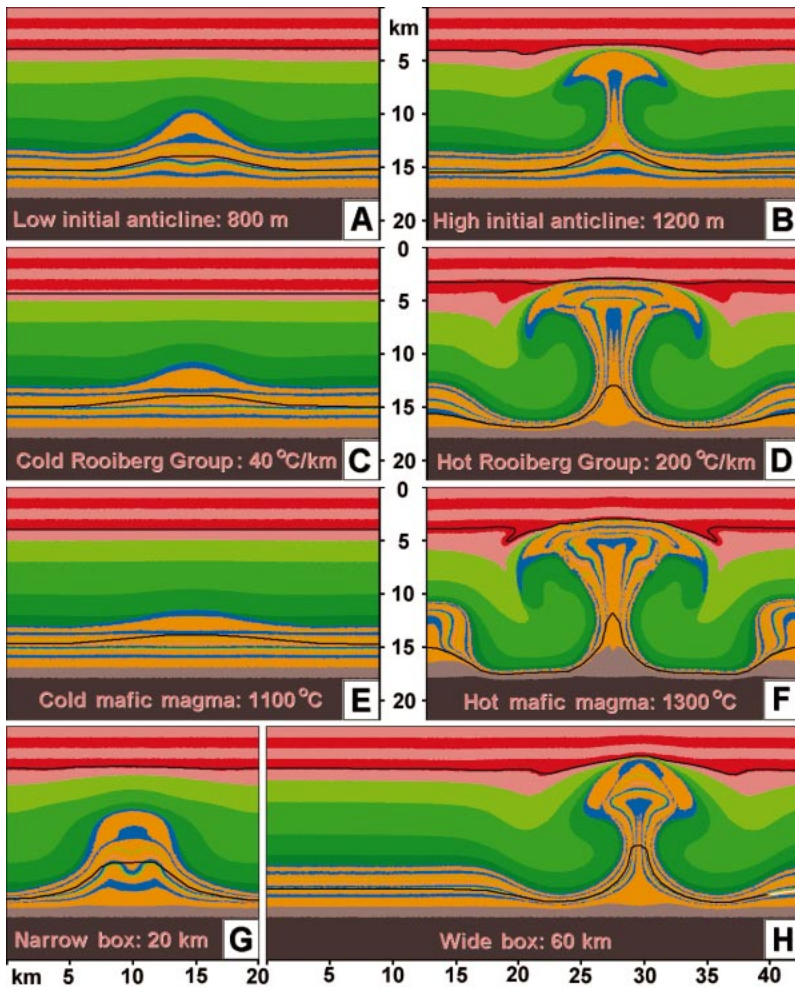


**Figure 3.** Changes in final geometry of diapir (cf. Fig. 2, bottom left panel) with changing numerical model parameters (see Table 1). A and B: Changes in height of initial anticline (A, 800 m; B, 1200 m). C and D: Changes in temperature distribution within Rooiberg Group (C, 25–225 °C and  $\partial T/\partial z = 40$  °C/km; D, 25–1025 °C and  $\partial T/\partial z = 200$  °C/km). E and F: Changes in emplacement temperature of Rustenburg Layered Suite (E, 1100 °C; F, 1300 °C). G and H: Changes in lateral box size (G, 20 km; H, 60 km [leftmost 43 × 22 km section of original 60 × 22 km symmetric model box is shown]). Other model parameters and colors as in Figure 2.

other mafic intrusions, provided they were large enough to furnish the necessary thermal energy and were endowed with the critical bottom topography indicated by our modeling (cf. Fig. 3). Moreover, similar thermomechanical phenomena may be anticipated in other natural settings characterized by an inverted vertical temperature gradient (i.e., by a decrease in temperature with depth). Apart from well-known double-diffusive convection phenomena in magma chambers and salt fingers in the oceans (e.g., Hansen and Yuen, 1990), such a situation exists in the proximity of subducting slabs. Diapirs and plumes of hydrated, partially molten subducted and/or mantle material generated in the proximity of the upper interface of the subducting slab at depths >100 km have been proposed and described

(e.g., Hall and Kincaid, 2001; Tamura et al., 2002). However, rather than being hot features in the classical sense, most of these are likely to be cold diapirs (Tamura, 1994; Gerya and Yuen, 2002), analogous to the structures described for the Bushveld Complex. Therefore, the diapiric features observed in the Bushveld Complex provide a unique opportunity for studying fossil evidence of the cold diapir phenomenon and can lead to a broader recognition and understanding of this process.

#### ACKNOWLEDGMENTS

We appreciate discussions with J. Van Decar concerning the cold diapir phenomenon. Supported by Russian Foundation of Basic Research grant 03-05-64633, the University of Natal Research Fund, an Alexander von Humboldt Foundation Research Fellowship (to Gerya), and the German Research So-

ciety under the auspices of Collaborative Research Center 526. Constructive reviews by C. Beaumont and S. Ellis are greatly appreciated.

#### REFERENCES CITED

- Bittner, D., and Schmeling, H., 1995, Numerical modeling of melting processes and induced diapirism in the lower crust: *Geophysical Journal International*, v. 123, p. 59–70.
- Cawthorn, R.G., Cooper, G.R.J., and Webb, S.J., 1998, Connectivity between the western and the eastern limbs of the Bushveld Complex: *South African Journal of Geology*, v. 101, p. 291–298.
- Du Plessis, A., and Kleywegt, R.J., 1987, A dipping sheet model for the mafic lobes of the Bushveld Complex: *South African Journal of Geology*, v. 90, p. 1–6.
- Gerya, T.V., and Yuen, D.A., 2002, Rayleigh-Taylor instabilities drive “cold plumes” at subduction zones: *Eos (Transactions, American Geophysical Union)*, v. 83, abs. T22A-1140, p. F1387.
- Gerya, T.V., Perchuk, L.L., Van Reenen, D.D., and Smit, C.A., 2000, Two-dimensional numerical modeling of pressure-temperature-time paths for the exhumation of some granulite facies terrains in the Precambrian: *Journal of Geodynamics*, v. 30, p. 17–35.
- Hall, P.S., and Kincaid, C., 2001, Diapiric flow at subduction zones: A recipe for rapid transport: *Science*, v. 292, p. 2472–2475.
- Hansen, U., and Yuen, D.A., 1990, Nonlinear physics of double-diffusive convection in geological systems: *Earth-Science Reviews*, v. 29, p. 385–399.
- Harmer, R.E., and Armstrong, R.A., 2000, Duration of Bushveld Complex (sensu lato) magmatism: Constraints from new SHRIMP zircon chronology: National Research Foundation, Bushveld Complex Workshop, Gethlane Lodge, South Africa, Abstracts, p. 11–12.
- Hatton, C.J., and Schweitzer, J.K., 1995, Evidence for synchronous extrusive and intrusive Bushveld magmatism: *Journal of African Earth Sciences*, v. 21, p. 579–594.
- Ramberg, H., 1981, Gravity, deformation and geological application: New York, Academic Press, 452 p.
- Ranalli, G., 1995, Rheology of the Earth (second edition): London, Chapman and Hall, 413 p.
- Sharpe, M.R., 1986, Eastern Bushveld Complex excursion guidebook: Extended abstracts, Geocongress '86: Johannesburg, Geological Society of South Africa, 135 p.
- Tamura, Y., 1994, Genesis of island arc magmas by mantle-derived bimodal magmatism: Evidence from the Shirahama Group, Japan: *Journal of Petrology*, v. 35, p. 619–645.
- Tamura, Y., Tatsumi, Y., Zhao, D.P., Kido, Y., and Shukuno, H., 2002, Hot fingers in the mantle wedge: New insights into magma genesis in subduction zones: *Earth and Planetary Science Letters*, v. 197, p. 105–116.
- Turcotte, D.L., and Schubert, G., 1982, Geodynamics: Application of continuum physics to geological problems: New York, John Wiley, 450 p.
- Uken, R., and Watkeys, M.K., 1997, Diapirism initiated by the Bushveld Complex, South Africa: *Geology*, v. 25, p. 723–726.

Manuscript received 10 February 2003  
 Revised manuscript received 21 May 2003  
 Manuscript accepted 25 May 2003

Printed in USA